APPLICATIONS OF ADVANCED SCALING FFAG ACCELERATOR

JB. Lagrange*[1)], T. Planche[1)], E. Yamakawa[1)],
Y. Ishi[2)], Y. Kuriyama[2)], Y. Mori[2)], K. Okabe[2)], T. Uesugi[2)],
[1)]Graduate School of Engineering, Kyoto University, Kyoto, Japan
[2)]Kyoto University Research Reactor Institute, Kumatori, Japan

Abstract

Until today, scaling FFAG accelerator were only designed in a ring shape. But a new criteria of the magnetic field configuration satisfying the scaling condition even for straight FFAG beam line is described here. Moreover, combining different types of cells can be used to imagine new lattices. Various applications using these recent developments are here examined: inprovements of the PRISM project and the ERIT project, and a zero-chromatic carbon gantry concept are presented.

INTRODUCTION

Recent developments in scaling FFAGs have opened new ways for lattice design [1, 2]. Indeed, it is possible to guide particles with no overall bend in scaling FFAGs, with an exponential field law. Different types of cells can be combined in the same lattice. It offers possibilities in terms of shape for rings and transport lines, but also leads to the creation of new functions, such as dispersion suppressors. This concept can be applied to overcome problems like in the PRISM project, or to improve existing schemes, like the ERIT lattice. Finally, a scaling FFAG carbon gantry concept is briefly described.

SCALING LAW

The scaling condition gathers two hypotheses:

- similarity of the closed orbits,
- similarity of the betatron oscillations, i.e. zero-chromaticity of the system.

To deal with the betatron oscillations, we use the linearized equations of motion around a closed orbit for a given momentum:

$$\begin{cases} \dfrac{d^2x}{ds^2} + \dfrac{1-n}{\rho^2}x = 0 \\ \dfrac{d^2z}{ds^2} + \dfrac{n}{\rho^2}z = 0 \end{cases}, \tag{1}$$

with ρ the curvature radius, s the curvilinear abscissa, x and z the perpendicular displacement off the closed orbit respectively in horizontal and in vertical and n the field index defined as

$$n = -\frac{\rho}{B}\left(\frac{\partial B}{\partial x}\right)_{z=0}. \tag{2}$$

* lagrange@rri.kyoto-u.ac.jp

To satisfy the scaling condition, Eq. (1) has then to be independent of momentum.

In circular elements, we start from a set of closed orbits for each momentum lying in the median plane. In this case, similarity of the closed orbits means that each of them is a photographic enlargement of each other. The general form of the vertical component of the magnetic field B in the mid-plane is[3, 4]

$$B = B_0\left(\frac{r}{r_0}\right)^k \mathcal{F}(\theta), \tag{3}$$

with r and θ the polar coordinates, B_0 the magnetic field at the radius r_0, $\mathcal{F}$ an arbitrary periodic function, and k the geometrical field index.

While in circular elements, the concept of closed orbit is obvious, the corresponding notion of reference trajectory in straight elements has first to be defined. A reference trajectory of a straight cell is a trajectory followed by a particle whose coordinates (i.e. angle and position) are the same at the entrance and at the exit of the cell.

In the same way than in circular elements, we start from a set of reference trajectories for each momentum lying in the median plane. In this case, similarity of the reference trajectories means that each of them is a translation of each other. Each reference trajectory is specified by its average abscissa X over one cell.

The betatron oscillations are invariant in momentum if Eq. (1) is the same for every momentum, and since s is independent of momentum, the condition to have invariant betatron oscillations is

$$\begin{cases} \dfrac{\partial}{\partial p}\left(\dfrac{1}{\rho^2}\right) = 0 \\ \dfrac{\partial}{\partial p}\left(\dfrac{n}{\rho^2}\right) = 0 \end{cases}. \tag{4}$$

The similarity condition of the reference trajectories validates the first equation of the system (4), since it gives that the curvature radius depends only on s, so is independent of momentum. We now focus on the second equation of the system (4).

If we differentiate the equation $p = qB\rho$, for a particle of momentum p and charge q, with respect to x, we have:

$$B\frac{\partial \rho}{\partial x} + \rho\frac{\partial B}{\partial x} = \frac{1}{q}\frac{dp}{dx} \tag{5}$$

If we introduce the field index n in Eq. (5), we have:

$$n = \frac{\partial \rho}{\partial x} - \frac{\rho}{p}\frac{dp}{dx}. \tag{6}$$

To express Eq. (6) in the coordinates (X, s), we now introduce the parameters η and ϵ that link dx with ds:

$$\eta = dx/dX, \quad (7)$$
$$\epsilon = ds/dX. \quad (8)$$

Then, rewriting Eq. (6) with η and ϵ, we get

$$n = -\frac{1}{\eta}\left(m\rho + \epsilon\frac{d\rho}{ds}\right), \quad (9)$$

with m a parameter given by

$$m = \frac{1}{p}\frac{dp}{dX}. \quad (10)$$

Rewriting m with the magnetic field B, we get:

$$m = \frac{1}{B}\frac{dB}{dX}. \quad (11)$$

In consequence, we have

$$\frac{n}{\rho^2} = -\frac{1}{\eta\rho}\left(m + \frac{\epsilon}{\rho}\frac{d\rho}{ds}\right). \quad (12)$$

The similarity gives that ρ, η and ϵ depend only on s, therefore they are independent of momentum. So, starting from the similarity of the reference orbits, The betatron oscillations are independent of momentum if and only if m is independent of momentum. In this case, we can integrate Eq. (11) and with the initial condition $B(X_0) = B_0$, we obtain the scaling law:

$$B = B_0 e^{m(X-X_0)}\mathcal{F}(s), \quad (13)$$

where $\mathcal{F}$ is an arbitrary periodic function.

As a remark, in the linear approximation, the field index n can be written in the circular section as

$$n = \frac{\rho}{r_0}k, \quad (14)$$

and in the straight section as

$$n = m\rho. \quad (15)$$

INSERTIONS AND DISPERSION SUPPRESSOR PRINCIPLE

Matching of reference trajectories

FFAG straight sections could be used with circular FFAG sections, but since field laws in each section are different, it will occur a discontinuity of reference trajectories at the border of these two sections. Before combining them together, it is useful to consider them separately. In scaling FFAG, the periodic dispersion function D of a cell for a given momentum p_0 is defined as

$$D_{circ.}(p_0) = p_0\left(\frac{\partial r}{\partial p}\right)_{p_0} = \frac{r}{k+1} \quad (16)$$

in circular elements, with r the radius of the closed orbit, and k the geometrical field index of the cell, and

$$D_{str.}(p_0) = p_0\left(\frac{\partial a}{\partial p}\right)_{p_0} = \frac{1}{m} \quad (17)$$

in straight elements, with a the abscissa of the reference trajectory and m the factor in the exponential law we discussed in Sec. .

In consequence, to combine a straight section and a circular section, after matching a special momentum p_0, dispersion can be matched with

$$m = \frac{k+1}{R_0}, \quad (18)$$

with R_0 the radius of the closed orbit for the momentum p_0 at the border of the cell in the circular section. But this matching is done only to the first order in $\frac{R-R_0}{R_0}$, with R the radius of the closed orbit for a momentum p at the border of the cell in the circular section. Higher orders effects create a reference trajectory mismatch for momenta other than p_0[1]. By a proper choice of p_0, the mismatch could be minimized for the considered momentum range. An example has been computed by simulating the insertion of straight sections in the 150 MeV FFAG ring of KURRI, for kinetic energies between 20 MeV and 150 MeV. The mismatch x as a function of kinetic energy is presented in Fig. 1. This maximum mismatch is around one cm for this case. It would be smaller for larger rings.

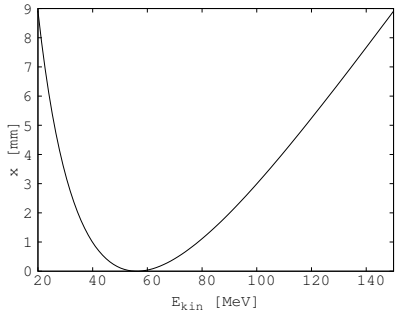

Figure 1: Mismatch of reference trajectories between circular cells and straight cells in 150 MeV FFAG ring example.

In the same way, it is possible to match two circular FFAG sections with different radii r_1 and r_2. The dispersion matching condition is kept by adjusting the geometrical field index:

$$\frac{k_1+1}{r_1} = \frac{k_2+1}{r_2}. \quad (19)$$

Matching of linear parameters

Once the reference trajectories are matched, the periodic beta-functions of the cells have also to be matched to limit the amplitude of the betatron oscillations. If a correct matching is not achievable, then an insertion with a phase advance multiple of 180 deg can be done for one of the

two different types of cells. This insertion becomes thus transparent, limiting the betatron oscillations.

Dispersion Suppressor

In FFAGs, dispersion suppressors can be useful at the end of a transport line, or to reduce excursion where rf cavities are set in FFAG rings. The effect of a dispersion suppressor would be to decrease the excursion, i.e. to bring closer the reference trajectories around a matched one. This excursion reduction can even be a complete suppression (see Fig. 2).

A principle of a dispersion suppressor in scaling FFAGs is presented in Fig. 2. The components of this scheme are three types of scaling FFAG cells, straight or circular. The area 1 contains FFAG cells with a dispersion D_1 at the border, the area 2, constituting the dispersion suppressor itself, contains FFAG cells with a dispersion D_2 at the borders, and the area 3 contains FFAG cells with a dispersion D_3 at the border. The conditions to have a dispersion suppressor are a phase advance of 180 deg. for the cells of the area 2 and the dispersion D_2 has to verify

$$D_2 = \frac{D_1 + D_3}{2}. \qquad (20)$$

This principle is based on the linear theory, so is valid as long as the effect of non-linearities is negligible.

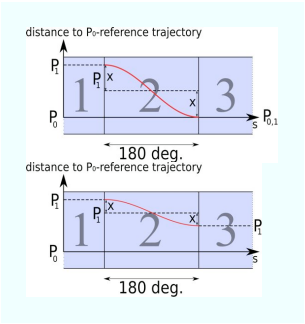

Figure 2: Principle of a dispersion suppressor with scaling FFAG cells. The upper scheme shows the case of a complete suppression of the dispersion, the lower one the case of a remaining dispersion after the dispersion suppressor.

PRISM CASE

The PRISM (Phase Rotated Intense Slow Muon beam) project aims to realize a low-energy muon beam with a high-intensity, narrow energy spread and high purity. For this purpose, a scaling FFAG ring has been proposed [5]. Requirements for the FFAG ring include a large transverse and longitudinal acceptance. The original design of the FFAG ring for PRISM is based on 10 identical DFD triplets. If this design fulfills the requirements of acceptance, the excursion is very large and the injection and extraction still remains difficult. To solve this problem, we consider the use of straight cells in the lattice and a new design is proposed (see Fig. 3). Parameters are summarized in table 1.

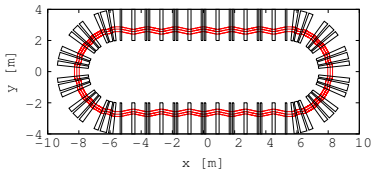

Figure 3: Closed orbits of 55 MeV/c, 68 MeV/c and 82 MeV/c muons μ^- in the PRISM lattice with straight sections.

Table 1: Parameters of the new PRISM lattice.

	Circular Section	**Straight Section**
Type	FDF	FDF
k-value or m-value	2.55	1.3 m^{-1}
Radius/Length	2.7 m	1.8 m
Horizontal phase advance	60 deg.	27 deg.
Vertical phase advance	90 deg.	97 deg.
Number of cells	2	3

Particle tracking is done with Runge-Kutta integration in soft edge fields with linear fringe field falloffs. Components of the field off the mid-plane are obtained from a first order Taylor expansion, satisfying the Maxwell equations.

The original PRISM design has a very large dispersion function ($\sim$ 1.2 m) that makes difficult the injection and the extraction. The new proposal starts then from a smaller one ($\sim$ 0.8 m). After minimizing the mismatch of the beta-functions, the bending part of the ring is made transparent to limit the effect of the remaining mismatch on the amplitude of the betatron oscillations. The resulting beta-functions for a momentum of 68 MeV/c are presented in Fig. 4. The working point is chosen in the tune diagram so that it is far from the structural normal resonances. The present working point has a tune of 2.9 in horizontal and 6.3 in vertical.

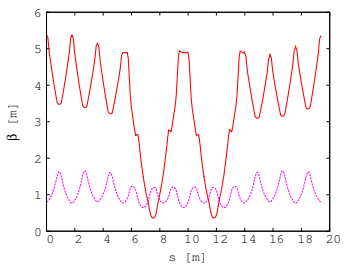

Figure 4: Horizontal (plain red) and vertical (dotted purple) beta-functions for half of the ring of the PRISM lattice.

The transverse acceptance in both planes is studied by tracking over 30 turns a particle with a displacement off the closed orbit and a small deviation in the other transverse direction (1 mm). Collimators ($\pm$ 1 m in horizontal, $\pm$ 30 cm in vertical) are used to identify the lost particles. The regions drawn by the particle with the largest initial stable amplitude in the horizontal and vertical phase spaces are respectively presented in Fig. 5 and 6. Horizontal ($\sim$ 24000 π.mm.mrad) and vertical ($\sim$ 6000 π.mm.mrad) acceptances are then measured by the area of the biggest ellipse included in this region.

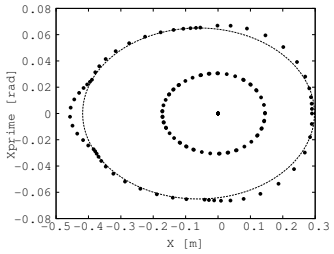

Figure 5: Horizontal phase space. Two particles with an initial displacement of 15 cm and 29 cm are tracked in the PRISM lattice over 30 turns. The dotted ellipse is the one used to measure the acceptance in the middle of the straight section.

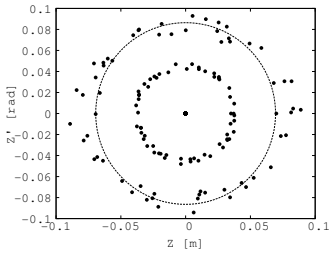

Figure 6: Vertical phase space. Two particles with an initial displacement of 3.5 cm and 7 cm are tracked in the PRISM lattice over 30 turns. The dotted ellipse is the one used to measure the acceptance in the middle of the straight section.

ERIT CASE

The ERIT (Energy/Emittance Recovery Internal Target) project with a scaling type of FFAG proton storage ring has been proposed as an accelerator-based intense thermal or epithermal neutron source (ABNS) for boron neutron capture therapy and constructed in KURRI [6]. Emittance blow up due to multiple scattering and energy straggling in the target is limited by ionization cooling. The results are promising [7], but since limitation of the survival rate of the protons comes from the emittance growth in the vertical plane, an insertion with a minimum of vertical betafunction could improve this scheme.

The purpose of the insertion is to decrease the value of the vertical betafunction at the target. In the existing scheme, the vertical betafunction is 0.8 m. The length of the insertion is settled from the RF frequency of the existing cavity (18.2 MHz). To minimize the effect of the mismatch on the amplitude of the betatron oscillations, the arc is modified by changing the k-value (from 1.92 to 2.57) to become transparent. This change in the design will have a small effect on dispersion (from 0.8 m to 0.65 m). The parameters of the new lattice are presented in table 2.

Table 2: Parameters of the new ERIT lattice.

	Circular Section	**Straight Section**
Type	FDF	DFFD
k-value or m-value	2.57	1.52 m^{-1}
Radius/Length	2.35 m	1.4 m
Horizontal phase advance	90 deg.	41 deg.
Vertical phase advance	90 deg.	148 deg.
Number of cells	8	2

Particle tracking is done again with Runge-Kutta integration in the same conditions than in the PRISM case. The tune is 2.22 in horizontal and 2.82 in vertical.

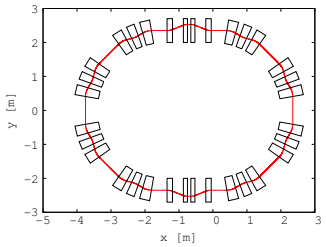

Figure 7: Closed orbit of 11 MeV proton in the ERIT lattice with the insertion.

Betafunctions are obtained with a small amplitude motion (see Fig. 8): at the target, the horizontal betafunction is 3.2 m and the vertical one 0.29 m. The vertical betafunction is thus smaller by a factor 3 at the target, but the horizontal one is bigger by a factor 2.5 compared with the original lattice. Further study must be realized to check if the horizontal acceptance (more than 10000π mm.mrad, see Fig. 9) is enough to handle the overheating due to the increase of the betafunction.

TRANSPORT LINE AND CARBON GANTRY

FFAG transport line could be useful to transport different momenta in a short time in the same line, like in hadron therapy gantries. In zero-chromatic FFAGs, each momentum has a different reference trajectory. Dispersion suppressors are then necessary at the beginning and at the end of the gantry since all different momenta come from and ar-

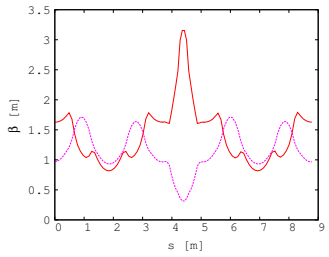

Figure 8: Horizontal (plain red) and vertical (dotted purple) beta-functions for half of the ring of the ERIT lattice.

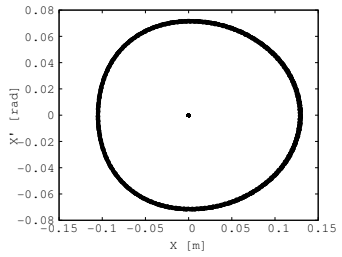

Figure 9: Horizontal phase space. An 11 MeV proton with an initial displacement of 13 cm is tracked in the ERIT lattice over 1000 turns.

rive at the same point. Another constraint comes from the reverse bend in the line. It induces to reverse the dispersion between the two bends, or to use a negative-k lattice in one of the bends. A schematic layout is presented in Fig. 10.

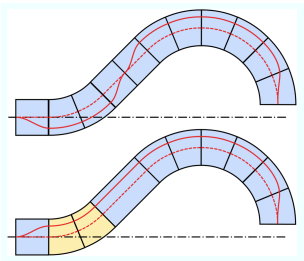

Figure 10: Schematic layout of a zero-chromatic FFAG gantry. The dotted red line represents the trajectory of a middle momentum, and the plain red line the maximum momentum. The mixed lines represents the rotation axis. The upper scheme shows the case of a reverse dispersion, the lower one the case of a negative-k lattice (in yellow).

SUMMARY

To overcome the problem of injection/extraction in the PRISM project, a new lattice using straight sections is proposed. An improvement of the ERIT scheme is then presented with a low-betafunction insertion in the ring. Finally the concept of a zero-chromatic FFAG carbon gantry is described. if these proposals need further studies, they open a promising way to improve lattices and schemes.

REFERENCES

[1] JB. Lagrange et al, "Straight section in scaling FFAG accelerator", PAC'09, Vancouver, FR5PFP002 (2009).

[2] JB. Lagrange et al, "Zero-chromatic FFAG straight section", FFAG'09, Fermilab (2009).

[3] K. R. Symon *et al., Phys. Rev.* **103**, *1840-1842 (1956).*

[4] A. A. Kolomensky and A. N. Lebedev, Theory of Cyclic Accelerators, (North-Holland, Amsterdam, 1966).

[5] "The PRISM Project - A Muon Source of the World-Highest Brightness by Phase Rotation -, LOI for Nuclear and Particle Physics Experiments at the J-PARC 217 (2003).

[6] Y. Mori, "Development of FFAG accelerators and their applications for intense secondary particle production", Nucl. Instrum. Methods Phys. Res. , Sect. A 562, 591-595 (2006).

[7] K. Okabe et al, "Study for FFAG-ERIT neutron source", IPAC'10 , Kyoto (2010).